Fast and Scalable Parallel External-Memory Construction of Colored Compacted de Bruijn Graphs with Cuttlefish 3

Jamshed Khan[1 [0000−0002−5129−9749]],
Laxman Dhulipala[1 [0000−0003−0685−064X]], and
Rob Patro[1 [0000−0001−8463−1675]]

Department of Computer Science, University of Maryland, MD 20742, USA
corresponding authors: jamshed@cs.umd.edu, rob@cs.umd.edu

Abstract. The rapid growth of genomic data over the past decade has made scalable and efficient sequence analysis algorithms, particularly for constructing de Bruijn graphs and their colored and compacted variants critical components of many bioinformatics pipelines. Colored compacted de Bruijn graphs condense repetitive sequence information, significantly reducing the data burden on downstream analyses like assembly, indexing, and pan-genomics. However, direct construction of these graphs is necessary as constructing the original uncompacted graph is essentially infeasible at large scale. In this paper, we introduce Cuttlefish 3, a state-of-the-art parallel, external-memory algorithm for constructing (colored) compacted de Bruijn graphs. Cuttlefish 3 introduces novel algorithmic improvements that provide its scalability and speed, including optimizations to significantly speed up local contractions within subgraphs, a parallel algorithm to join local solutions based on parallel list-ranking, and a sparsification method to vastly reduce the amount of data required to compute the colored graph. Leveraging these algorithmic strategies along with algorithm engineering optimizations in parallel and external-memory setting, Cuttlefish 3 demonstrates state-of-the-art performance, surpassing existing approaches in speed and scalability across various genomic datasets in both colored and uncolored scenarios.

1 Introduction

A fundamental object for analyzing high-throughput genomic data (both raw sequencing reads and assembled genomes) is the de Bruijn graph and its variants. The many uses of this elegant combinatorial object throughout bioinformatics are too numerous to enumerate here, but they span a wide gamut, from assembly, variant mapping, and sequence-similarity search, to pangenome analysis.

Given a set of sequences, each distinct k-mer that is a substring of some input sequence forms a vertex in the de Bruijn graph and each (k+1)-mer forms an edge between its prefix and its suffix k-mers. Thus an input sequence corresponds to a unique walk in the graph. The compacted variant of the de Bruijn graph is obtained by collapsing each maximal non-branching path of the original graph into individual meta-vertices. However, by collapsing all the occurrences of the same k-mer into a single vertex and discarding their "source"-labels, the (compacted) de Bruijn graph loses the source-information for the vertices. The *colored* variant of a de Bruijn graph associates a "color" to each vertex, which is the set of input sequences where the corresponding k-mer is present in—i.e. the colored variant adds an inverted index to the graph. On related genomic data, the number of vertices in the compacted graph tends to be *orders of magnitudes smaller* than the original graph [19], which can vastly improve the time- and memory-efficiency of downstream applications.

In this paper, we study the fundamental question of whether it is possible to scale the construction of (colored) compacted de Bruijn graphs to very large datasets while obtaining scalable high performance and low resource requirements. This question is critical as many computational genomics workflows employing these graphs are multi-phased, and generally the most computationally intensive phase is the initial one of constructing the graph. Despite significant recent progress on improved algorithms for building these graph variants [6,24,20,19], existing methods still struggle to scale to extremely large and highly redundant datasets within feasible timing requirements, and obtaining faster algorithms would directly speed up numerous downstream applications.

Our main contribution in this paper is Cuttlefish 3, a new algorithm for parallel, highly-scalable, and time- and memory-efficient construction of the (colored) compacted de Bruijn graph. Cuttlefish 3 makes

significant algorithmic improvements to our previous approaches (Cuttlefish [20] and Cuttlefish 2 [19]) to reduce the amount of computational work performed, resulting in better absolute performance. It also makes more careful use of external-memory to reduce the memory-requirement of the algorithm without compromising scalability. In contrast to its predecessors, Cuttlefish 3 adopts the paradigm [6,7] of first partitioning the data into nearly-disjoint subgraphs, performing local contraction (with color-set tracking and aggregation, if applicable) within each of these subgraphs, and then joining together their locally-maximal unitigs into the globally complete (colored) compacted graph. Ultimately, we believe that this general paradigm is likely to be an optimal approach to the problem, at least in the limit as the data grows increasingly large. Nonetheless, our results show that there are *substantial* opportunities for improvement over the current state-of-the-art manifestation of this paradigm, GGCAT [9].

Our new results are obtained through novel algorithmic ideas and careful algorithm engineering optimizations which we believe may be of independent interest. Three of our highlights include: (1) a technique for reducing the number of graph-membership queries when constructing locally-maximal unitigs; (2) a novel color-set collection scheme by extracting the color information of a very sparse set of vertices using a combinable hash of the source identifiers; and (3) a new deterministic and highly parallelizable algorithm for the global stitching phase based on parallel list-ranking.

These ideas yield significant performance improvements as a whole for the (colored) compacted de Bruijn graph construction. For example, our color extraction technique is based on identifying a sparse subset of *color-shifting* vertices (ones which have a different color from their immediate neighbor). By only constructing full color-sets for a subset of the color-shifting vertices, we show that we can obtain the color-sets of all the vertices while drastically reducing the amount of information that must be shuffled and sorted compared to the naive approach of simply collecting and sorting all k-mer–color pairs.

In the rest of this paper, we describe the design of Cuttlefish 3 and elaborate more on our algorithmic techniques and performance engineering contributions. Due to space constraints, we provide additional details and proofs in the Supplementary Materials.

Preliminaries. We assume all symbols to belong to the alphabet $\Sigma = \{A, C, G, T\}$. A *string* s is an ordered sequence of symbols drawn from Σ. $|s|$ denotes the length of s. s_i denotes the i'th symbol in s with 0-indexing. The *substring* $s_{i..j}$ of s is the string located within s from its i'th to the j'th indices, exclusive of the index j. The ℓ-length *prefix* of s is $\mathtt{pre}_\ell(s) = s_{0..\ell}$, and the ℓ-length *suffix* of s is $\mathtt{suf}_\ell(s) = s_{|s|-\ell..|s|}$. The *append* operation is denoted by $\cdot$. For two strings x and y such that $\mathtt{suf}_\ell(x) = \mathtt{pre}_\ell(y)$, the ℓ-*glue* operation $\odot^\ell$ produces the string $x \odot^\ell y = x \cdot y_{\ell..|y|}$. A k-*mer* is a k-length string.

Each symbol in Σ has a reciprocal *complement*—the complementary pairs being (A, T) and (C, G). For a symbol c, $\bar{c}$ denotes its complement. For a string s, its *reverse-complement* $\bar{s}$ is the string of the complemented symbols of s in the reverse order, i.e. $\bar{s} = \bar{s}_{|s|-1} \cdot \ldots \cdot \bar{s}_0$. The *canonical* form of s is $\hat{s} = \min(s, \bar{s})$, per some strict total order of $\Sigma^{|s|}$. We lexicaly order strings.

The *frequency* $f(x, \mathcal{S})$ of some string x in a multiset $\mathcal{S}$ of strings is the count of different instances of x present as substrings across all $s \in \mathcal{S}$. Its *canonical frequency* is defined as $\hat{f}(x, \mathcal{S}) = f(x, \mathcal{S}) + f(\bar{x}, \mathcal{S})$.

Given a multiset $\mathcal{S}$ of strings, an integer $k > 0$, and a frequency threshold f_0, let $\mathcal{K}_{+1}$ be the set of $(k+1)$-mers e with $f(e, \mathcal{S}) \geq f_0$. The *(edge-centric) directed de Bruijn graph of order* k of $\mathcal{S}$ is a graph $G = (\mathcal{V}, \mathcal{E})$ such that each $e = u \odot^{k-1} v \in \mathcal{K}_{+1}$ is an edge from the vertex u to the vertex v. Thus $\mathcal{E} = \mathcal{K}_{+1}$ and $\mathcal{V}$ is induced by $\mathcal{E}$. For ease of notation, we use the terms k-mer and vertex and the terms $(k+1)$-mer and edge interchangeably.

The *bidirected de Bruijn graph* is an extension of the directed model. $\mathcal{E}$ is the set of $(k+1)$-mers e with $\hat{f}(e, \mathcal{S}) \geq f_0$. Each vertex represents two k-mers, u and $\bar{u}$, and is denoted with $\hat{u}$. It has two *sides*: $\mathtt{front}$ and $\mathtt{back}$. An edge $e = u \odot^{k-1} v$ is said to *exit* $\hat{u}$ and *enter* $\hat{v}$. e exits $\hat{u}$ through its $\mathtt{back}$ iff $u = \hat{u}$, and it enters $\hat{v}$ through its $\mathtt{front}$ iff $v = \hat{v}$. The opposite sides are used respectively in the other cases. Thus the edge $e = u \odot^{k-1} v$ is represented as $\big((\hat{u}, \sigma_u), (\hat{v}, \sigma_v)\big)$—it goes from the side σ_u of vertex $\hat{u}$ to the side σ_v of vertex $\hat{v}$. This edge is said to *spell* the $(k+1)$-mer $u \odot^{k-1} v$. The $(k+1)$-mer $\bar{e} = \bar{v} \odot^{k-1} \bar{u}$ induces the edge $\big((\hat{v}, \sigma_v), (\hat{u}, \sigma_u)\big)$—it mirrors e in the opposite direction [19]. For some side σ, $\bar{\sigma}$ denotes the opposite side.

A *walk* $w = (\widehat{v_0}, e_1, \widehat{v_1}, \ldots, \widehat{v_{n-1}}, e_n, \widehat{v_n})$ is an alternating sequence of vertexes v_i and edges e_j such that any two successive edges are of the form $e_j = \big((\hat{x}, \sigma_x), (\hat{y}, \sigma_y)\big)$ and $e_{j+1} = \big((\hat{y}, \bar{\sigma_y}), (\hat{z}, \sigma_z)\big)$. That is, a walk enters and exits a vertex through different sides. Let e_i spell the $(k+1)$-mer s_i. Then w spells the string

$s_1 \odot^k \ldots \odot^k s_n$. If w is a singleton [1], then it spells the k-mer $\widehat{v_0}$. A *path* is a walk w without any repeated vertex, except possibly $\widehat{v_0} = \widehat{v_n}$, in which case it is also a *cycle*.

A *unitig* is a path $p = (\widehat{v_0}, e_1, \widehat{v_1}, \ldots, e_n, \widehat{v_n})$ such that either p is a singleton, or: (1) for each $0 < i < n$, the only edges incident to $\widehat{v_i}$ are e_i and e_{i+1}; and (2) the sides of $\widehat{v_0}$ and $\widehat{v_n}$ to which e_1 and e_n are incident to, respectively, do not have any other incident edge. A unitig is *maximal* if cannot be extended on either side. The problem of *de Bruijn graph contraction* is to compute all the maximal unitigs of the graph. See [19] for detailed examples of these constructs.

Given the multiset $\mathcal{S}$ of strings, a *color-set* (or simply, *color*) is a subset of $\mathcal{S}$. In a *colored de Bruijn graph*, each vertex v has an associated color $\{s \in \mathcal{S} : \widehat{f}(v, s) > 0\}$—each vertex maps to all the $s \in \mathcal{S}$ in which it is contained. For ease of the algorithm exposition, we redefine colors to be sets of integers: we index $\mathcal{S}$ as $\mathcal{S} = \{s_1, \ldots, s_n\}$ and define v's color as $\{i : \widehat{f}(v, s_i) > 0\}$.

Given some $\ell < k$ and a total ordering of ℓ-mers, the ℓ-*minimizer* $\mathtt{mm}(x)$ of a k-mer x is the smallest ℓ-mer substring of x. The *canonical* ℓ-*minimizer* of x is $\mu(x) = \min(\mathtt{mm}(x), \mathtt{mm}(\overline{x}))$. We define $\mathtt{lmm}(x) = \mu(\mathtt{pre}_{\ell-1}(x))$ and $\mathtt{rmm}(x) = \mu(\mathtt{suf}_{\ell-1}(x))$, the canonical ℓ-minimizer of the prefix and the suffix $(k-1)$-mers, respectively. x is said to be a *discontinuity* k-*mer* if $\mathtt{lmm}(x) \neq \mathtt{rmm}(x)$. A string s with $|s| \geq k$ is a *super* k-*mer* iff all its substring k-mers have the same canonical ℓ-minimizer. [2]

2 Algorithm Overview

We provide a high-level overview of CUTTLEFISH-3$(\mathcal{S}, k, f_0)$ in this section. The input is a set $\mathcal{S}$ of strings, an integer k, and a frequency threshold f_0. The output is the spellings of the maximal unitigs of the induced de Bruijn graph.

A simple algorithm to solve the problem is to first construct the original de Bruijn graph, and then to traverse the graph to find all the maximal non-branching paths. Unfortunately, this approach requires storing a representation of the graph *in-memory*, which quickly becomes infeasible at scale.

CUTTLEFISH 3 adopts the partition-contract-join paradigm in which the input data is (1) first *partitioned* into near-disjoint subsets (constituting subgraphs of the de Bruijn graph); (2) all maximal non-branching paths are *contracted* within these subgraphs; (3) and finally the local (per-subgraph) solutions are *joined* into the global solution. These high-level steps have been proposed in this context by [21,6], and later followed by [7,9].

```
CUTTLEFISH-3(S, k, f_0)
    // Partition G into a set 𝒢 of subgraphs
1   𝒢 = PARTITION-GRAPH(S, k)
    // Contract each subgraph 𝒢_i and construct the
       discontinuity graph Γ
2   Γ = CONTRACT-SUBGRAPHS(𝒢, f_0)
    // Contract Γ to meta-vertices
3   Π = CONTRACT-PATHS(Γ)
    // Expand back the meta-vertices to Γ and
       compute the edges' coordinates
4   χ = EXPAND-PATHS(Γ, Π)
    // Collate unitigs from the same path in proper rank
5   𝒫 = COLLATE-UNITIGS(Γ, χ)
6   return 𝒫
```

CUTTLEFISH 3 first implicitly partitions the graph G into subgraphs by distributing its edges, available from $\mathcal{S}$, to external-memory buckets using minimizers. Then each subgraph is loaded in-memory and separately contracted using a simple graph-traversal algorithm. The unitig set $\mathcal{U}$ produced from the subgraphs form partial results of the global problem.

During the local phase, another graph Γ, called the *discontinuity graph*, is constructed in external-memory. The vertices of Γ are the discontinuity k-mers from $\mathcal{S}$, i.e. it is a subset of the vertex-set of G, and each edge correspond to a unitig in $\mathcal{U}$. We show that Γ is a collection of disjoint maximal paths and that each one

[1] Only a single vertex.

[2] To bound the maximum lengths of super k-mers, we slightly abuse notation such that $\mathtt{mm}(x)$ also includes the offset of the minimizer in x, with ties broken in favor of the leftmost offset, and thus $\mu(x)$ also includes the offset.

corresponds to a maximal unitig of G. Thus traversing each disjoint path in Γ and collecting the edges in order provides the corresponding global maximal unitig.

At very large scale (e.g., for trillion-base genome collections), using an in-memory representation of Γ also requires substantial space. Instead, we model the problem of computing the coordinates of each edge, i.e. the path p it belongs to and its rank in p, as a *list-ranking* problem [28]. We propose a novel algorithm, inspired by seminal parallel algorithms for *tree-contraction* [23], to solve this problem efficiently in external-memory. Once the coordinates of the edges of Γ are available, the full paths, i.e. the global maximal unitigs, are constructed by joining the edges appropriately with a *MapReduce*-like [10] key-value collation scheme, also done in external-memory. Pseudocode for the different phases are provided in the Supplementary Material.

The next subsections describe the steps of the algorithm in more detail. Pseudocodes of different steps and proofs are present in the Supplementary Material. For ease of exposition, we describe the algorithm while skipping more involved details about handling vertex-sides. We emphasize that Cuttlefish 3 and its implementation do take vertex-sides into consideration.

2.1 Partitioning G Into Subgraphs

The de Bruijn graph G is first partitioned into a set $\mathcal{G}$ of 4^ℓ subgraphs, where $\ell < k$ is the chosen minimizer size, by assigning each induced edge $e = u \odot^{k-1} v$ from the input to the graph $\mathcal{G}_{\mathtt{rmm}(u)}$ (which is the same as $\mathcal{G}_{\mathtt{lmm}(v)}$). Each edge is thus assigned to a unique subgraph. Using a partitioning strategy similar to [7], each discontinuity k-mer is assigned as a vertex in exactly two subgraphs. Figure 1a provides an example illustration of such partitioning.

Instead of assigning each edge individually, Cuttlefish 3 assigns longer spans of *consecutive edges*, as induced by their enclosing super k-mers [21], from the input to subgraphs. All the edges from a super k-mer belong to the same subgraph (see Corollary 1). Given a string, all its maximal super k-mers can be computed in linear time using a monotonic queue [30]. We provide a linear time and more practically efficient (branch-free) algorithm for such in Section 3.1.

2.2 Contracting Each Subgraph

Once all input edges are distributed to the subgraphs in external-memory, a hash-table representation of the de Bruijn graph of each subgraph $\mathcal{G}_i$ is constructed in-memory. In the representation, the keys are the vertices (k-mers) and their associated values are the *states* (neighborhood encodings). Since de Bruijn graphs have bounded-degree, we generalize the vertex-state modeling from [20] to encode a vertex's complete adjacency information: frequency-encoding (or presence-absence) of all possible eight incident edges. Given the state of a vertex, its complete set of edges can be quickly inferred.

Once the in-memory representation of $\mathcal{G}_i$ is constructed, the algorithm initiates a non-branching walk from each side of every vertex x. A walk continues so long as, for each extension edge $e = \{(u, \sigma_u), (v, \sigma_v)\}$ from a vertex u, e is the *only* edge incident to the sides σ_u and σ_v. These two walks constitute the maximal unitig of x (and of all the other vertices in the walks). The majority of the work performed during this phase is spent querying the hash table while performing these walks. To extend a walk from u with edge $\{(u, \sigma_u), (v, \sigma_v)\}$, typical de Bruijn graph traversal strategies [9,15,17,8] require probing for the existence of all possible neighbors at σ_u and at σ_v—amounting to eight membership queries for each successful extension of such walks in the DNA alphabet. For unsuccessful extensions, i.e. branching or dead-end at σ_u or σ_v, at least two and up-to eight queries are used. In Cuttlefish 3, the vertex states in the hash table allows us to elide most of these queries when performing the walks. Specifically, using the neighborhood states of the vertices u and v, Cuttlefish 3 requires *only one query* in a successful extension from u through σ_u—whether or not σ_u or σ_v branch can be inferred from u and v's states; only v's state needs to be queried. For unsuccessful extensions, Cuttlefish 3 requires zero or one query: zero in the case where σ_u has no unique edge, and one otherwise, to fetch v's state. Thus, associating adjacency states to vertices reduces the expected number of membership queries by a constant factor—up to $8\times$ fewer queries compared to methods that query for all possible neighbors.

Discontinuity Graph Construction Let x be an endpoint of a maximal unitig p in $\mathcal{G}_i$ and σ_x be the side of x not connected to p. x terminates p due to one of the following reasons: (1) σ_x has 0 edges; or (2) σ_x

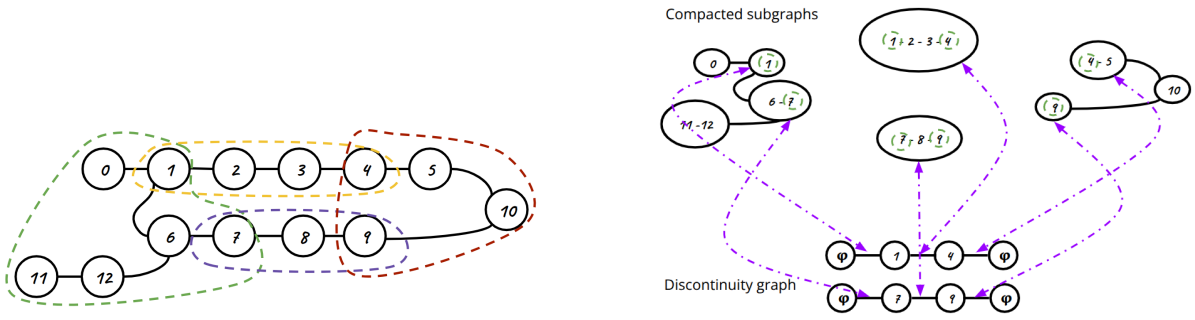

(a) (b)

Fig. 1: In (a), we show a sample partitioning of a de Bruijn graph G into subgraphs. Each set of vertices enclosed with dashed borders is a subgraph. In (b), we show the compacted subgraphs and the corresponding discontinuity graph. Maximal unitigs are collapsed into single vertices in the contracted subgraphs. Discontinuity vertices from the original graph are circled with dotted green border. These form the vertex set of the discontinuity graph Γ. Each local maximal unitig containing discontinuity vertex(es) correspond to an edge in Γ, shown with the dashed arrows. The maximal paths in Γ correspond to global maximal unitigs of G.

has > 1 edges; or (3) σ_x connects to a unique neighbor y's side σ_y which has > 1 edges. Maximal unitigs from $\mathcal{G}_i$ that have both their endpoints satisfying case (2) or (3) form maximal unitigs of G. Whereas in case (1), if x is a discontinuity vertex, i.e. it has different minimizers $i \neq j$ in its prefix and suffix $(k-1)$-mers, then the other vertices that would continue the underlying maximal unitig in the global graph G through σ_x are absent in $\mathcal{G}_i$ and present in $\mathcal{G}_j$. $\mathcal{G}_i$'s unitigs with endpoints having this property can be further extended in G but not in $\mathcal{G}_i$. Such local maximal unitigs appearing in *different subgraphs* need to be joined together appropriately to compute the correct global output. CUTTLEFISH 3 solves this problem through another graph Γ, defined from G, called the discontinuity graph.

Γ is a weighted and labeled graph with labels associated to each edge. Its vertex set is the set of discontinuity vertices from G. If a maximal unitig p in $\mathcal{G}_i$ has discontinuity endpoints x and y, an edge $\{x, y\}$ is added to Γ with weight 1 and the spelling of p as a label. In case either of x and y is not a discontinuity, a sentinel vertex ϕ is used in its place. Fig. 1b provides an example illustration of contracted subgraphs and the resultant discontinuity graph produced.

2.3 Joining Subgraph-local Maximal Unitigs

Discontinuity Graph Structure We prove that Γ is a collection of maximal disjoint paths (see Lemma 4). These maximal paths correspond to the maximal unitigs in G that span multiple subgraphs (see Lemma 5).

Consider a maximal path $p = (\phi, v_1, v_2, \ldots, v_n, \phi)$ in Γ corresponding to the maximal unitig u in G. Let the sequence of edges in p be $(e_1, e_2, \ldots, e_n, e_{n+1})$. Each e_i has a label u_i which is a local maximal unitig from some subgraph $\mathcal{G}_j$. As such, $u = u_1 \odot^{k-1} u_2 \odot^{k-1} \ldots \odot^{k-1} u_{n+1}$. Hence, if the edges e_i of p are known, then ordering the edges e_i appropriately and concatenating their labels u_i in that order will produce u. But the construction of Γ only produces its edge set $\{e : (\{x, y\}, 1, s)\}$ (see Sec. 2.2), and hence for some e_i, we know neither the ID of the maximal path p it belongs to, nor its rank i in p. We model this problem in detail as following.

Formulating a List-Ranking Problem Let $p = (\phi, v_1, v_2, \ldots, v_n, \phi)$ be a maximal path in Γ. For simpler exposition, let us differentiate its two instances of the sentinel vertex ϕ as $p = (v_0 = \phi_l, v_1, v_2, \ldots, v_n, v_{n+1} = \phi_r)$ [3]. Let p's edges in order be $(e_1, e_2, \ldots, e_n, e_{n+1})$. For each e_i, we need to compute the ID of this path p and its rank in p. The (0-based) rank of e_i in p's edges is $\texttt{rank}(e_i) = i - 1$,

[3] The ϕ vertex has rank 0 in all paths. The last vertex in a path having rank 0 forms a corner case in the rank computation of edges from its endpoints' ranks, and a special case with paths having two edges.

whereas the rank of v_i in p's vertices is $\texttt{rank}(v_i) = i$. Since $e_i = (\{v_{i-1}, v_i\}, _, _)$, $\texttt{rank}(e_i) = \texttt{rank}(v_{i-1})$. Thus we can solve for the vertices' ranks instead. Considering each maximal path p an ordered list, we need to compute for each vertex v, which list (path) it belongs to, $\texttt{path}(v)$, and at what rank, $\texttt{rank}(v)$—this is exactly the classical *list-ranking* problem [28].

Solving the List-Ranking Problem There exist parallel in-memory solutions [4] for the list-ranking problem. But with practical datasets at scale, this graph can become very large for an in-memory representation. Therefore, we design an external-memory solution for this problem instance, inspired from the algorithm design technique of *tree-contraction* [23]. The idea is to (in parallel) contract the list to a single vertex through a sequence of *compress* operations, which essentially contract sets of vertices into single vertices, and solve the problem of interest incrementally during contractions.

We aim to contract each maximal path p of Γ into a single vertex v through a series of contractions and solve the list-ranking problem for just v. Then, we aim to expand v back to p through a series of expansion operations, in the opposite order of the contraction operations, and solve the problem for the rest of the vertices of p along the way. We will perform these contraction and expansion operations in batches, keeping only a disjoint subset of the vertices and the edges of Γ in memory for each batch, thus avoiding a full in-memory graph representation.

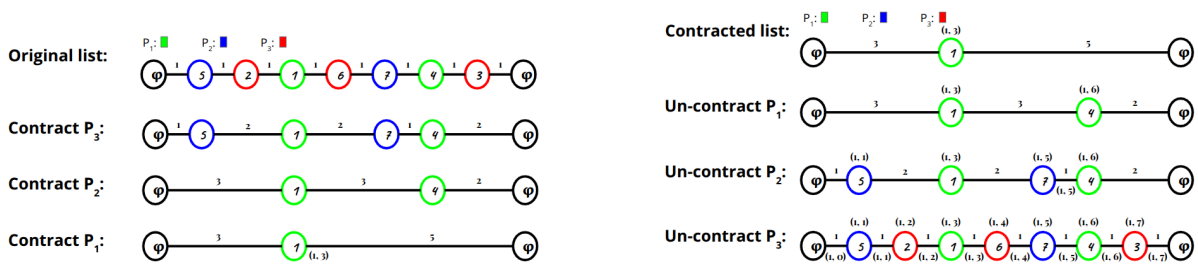

(a) Example execution of the contraction of a maximal path in Γ. The $v \in \Gamma$ are assigned to three partitions: P_1, P_2, and P_3. P_3 (red) and its incident edges are contracted first, producing a shorter list with only P_1 and P_2 vertices, and some newly added edges. Then P_2's (blue) vertices and edges are contracted, and finally of P_1's (green). Without producing a $\{\phi_l, \phi_r\}$ edge, a single vertex has to be kept in the final form of the list to retain the list's identity. Thus only vertex 1 survives, having edges to ϕ_l and ϕ_r with weights 3 and 5, respectively. The original list is assigned ID 1 (due to the sole vertex 1), and 1's rank is computed to be 3.

(b) Example execution of the expansion of a contracted path in Γ. Over each vertex is shown its (list ID, rank) pair. The contracted list has a single vertex 1 with list ID 1 and rank 3. P_1 is un-contracted first—rest of its vertices are reintroduced to the list, appropriately computing their ranks. Then P_2's vertices are reintroduced, and finally of P_3's. The unit-weight edges belong to the original form of the list, and their list ID and rank is also computed during reintroduction. These pairs are shown below the edges. When the entire original list is expanded back, all its edges' list IDs and ranks are known.

Fig. 2: Example contraction and expansion of a maximal path in Γ.

Discontinuity Graph Contraction We hypothetically partition the vertex set of Γ into n partitions—each vertex v belongs to a partition $\mathfrak{P}(v) \in [1, n]$ through uniform hashing, with $\mathfrak{P}(\phi_l) = \mathfrak{P}(\phi_r) = 0$. We load each partition $\mathcal{P}_i$ into memory, sequentially, in descending order from n to 1 (though any order would work) and contract each $v \in \mathcal{P}_i$ and their incident edges from Γ in parallel, as follows.

Suppose that a maximal path p has the form $(\ldots, x, y, z, \ldots)$ right before contracting partition $\mathcal{P}_i$. Then $\mathfrak{P}(v) \leq i$ for all $v \in p$, since all the partitions $\mathcal{P}_{j>i}$ have been contracted by this point. Say that y belongs to $\mathcal{P}_i$ but not x and z, i.e. $\mathfrak{P}(y) = i$, $\mathfrak{P}(x) < i$ and $\mathfrak{P}(z) < i$, and the edges between them are $e_{xy} = (\{x, y\}, w_{xy}, _)$ and $e_{yz} = (\{y, z\}, w_{yz}, _)$. Then we merge the edges e_{xy} and e_{yz} to a new edge $e_{xz} = (\{x, z\}, w_{xy} + w_{yz}, _)$. If there are successive vertices (y_j) in $p = (\ldots, x, y_1, \ldots, y_m, z, \ldots)$ with $\mathfrak{P}(y_j) = i$, then the entire chain of y_j is merged to a single edge e_{xz} having weight equal to the sum of the weights along the chain's edges.

This way all the edges incident to $\mathcal{P}_i$ are contracted in parallel and a smaller list is produced for the next step of contracting $\mathcal{P}_{i-1}$.

Finally, during contraction of $\mathcal{P}_i$, if some path p is found to be of the form (ϕ_l, y, ϕ_r), we set y to be the path-ID of p. Hence, $\texttt{path}(y) = y$ and $\texttt{rank}(y) = w_{\phi_l y}$, the weight of the $\{\phi_l, y\}$ edge. Since compacted de Bruijn graphs form a vertex-decomposition of the graph [7], y is uniquely present in this contracted path (and the original maximal path)—the strategy of assigning each maximal path in Γ the ID of one of its vertices as its list ID ensures uniqueness of the list IDs. The rank of y is correct by induction as all edges in the original path have unit weights and the contractions merge edges by summing their weights. Fig. 2a illustrates an example execution of this method.

Expansion of the Contracted Graph Now that for each maximal path, the path ID and the rank of a single vertex is computed, we use this partial solution incrementally to compute the solution for the rest of the vertices. We use an expansion (un-contraction) scheme that is complementary to the contraction process to expand back the contracted paths to their original forms. The algorithm loads each partition $\mathcal{P}_i$ into memory sequentially in the opposite order that the partitions were contracted, i.e. in ascending order from 1 to n. By induction, the path ID and the rank of each vertex in $\mathcal{P}_i$ have been computed at this point.[4] The base case of the induction is for $\mathcal{P}_1$—all its vertices' path IDs and ranks have been computed in the last step of contraction. Now during the i'th step of expansion, for each $v \in \mathcal{P}_i$, $\texttt{path}(v)$ and $\texttt{rank}(v)$ are propagated through its incident edges, including the ones introduced during the contractions, in parallel, as follows.

Say that for vertices x, y, and z, there exist edges $e_{xy} = (\{x, y\}, w_{xy}, _)$ and $e_{yz} = (\{y, z\}, w_{yz}, _)$. These edges may belong to the original path, or may have been introduced by the contractions. Suppose that $\mathfrak{P}(y) = i$, $\mathfrak{P}(x) > i$, and $\mathfrak{P}(z) > i$. Since y belongs to $\mathcal{P}_i$, its path ID and rank have been computed by now. Let these be $\texttt{path}(y) = \pi$ and $\texttt{rank}(y) = \rho$, respectively. Then during expansion from $\mathcal{P}_i$, e_{xy} and e_{yz} are reintroduced to some path p. The path ID and the ranks of x and z are computed as $\texttt{path}(x) = \texttt{path}(z) = \pi$, $\texttt{rank}(x) = \rho - w_{xy}$, and $\texttt{rank}(z) = \rho + w_{yz}$. Besides, if any of e_{xy} and e_{yz} has weight 1, then it is an original edge of Γ and we need its path ID and rank. As described in the list-ranking formulation, for such an edge $e = (\{u, v\}, 1, s)$, $\texttt{path}(e) = \texttt{path}(u)$ and $\texttt{rank}(e) = \texttt{rank}(u)$. The correctness of the computed path IDs and the ranks during expansion hold by induction. Fig. 2b illustrates an example execution of the method.

Discontinuity Graph Representation For the proposed path contraction and expansion strategies to work, we require the ability to load partitions of Γ into memory. Recall that, during subgraphs contraction (see Sec. 2.2), Γ is available as an edge-list. Edge-lists, as is, do not support loading edges only incident to a specific vertex partition without a complete scan. As such, we use a modified variant of the edge-list to represent Γ, which we refer as the *blocked edge-matrix*.

The blocked edge-matrix of Γ is an $(n+1) \times (n+1)$ matrix where each cell is an edge-list, which is a block (subset) of the actual edge-list. Each cell has an associated external-memory bucket for its edges. Consider an original edge $e = (\{x, y\}, 1, s)$ in Γ, and let $\mathfrak{P}(x) = p$ and $\mathfrak{P}(y) = q$. We add e to the (p, q) and the (q, p)'th cells of Γ. Newly introduced edges during contraction of Γ are also added to the matrix similarly. Thus when we need to access all the edges incident to partition i, we only load the edge-lists in either the i'th row or the i'th column of Γ.

We further reduce the external-memory requirement of this representation by half by adding e to only one cell. For $e = (\{x, y\}, w_{xy}, _)$, let $p = \mathfrak{P}(x)$ and $q = \mathfrak{P}(y)$. WLOG, assume $p \leq q$, otherwise we swap the endpoints. We add e only to the cell (p, q).

Recall that, during contraction, when processing $\mathcal{P}_j$, we only need access to the edges between $(\mathcal{P}_i, \mathcal{P}_j)$ for all $i \leq j$. Edges between $(\mathcal{P}_j, \mathcal{P}_k)$ for $k > j$ are not required as $\mathcal{P}_k$ has been contracted out by this point. Then it suffices to only load the cells (i, j) such that $i \leq j$—which are in the j'th column of Γ in its upper triangle. Similarly, during expansion, when processing $\mathcal{P}_i$, we require access to only the edges between $(\mathcal{P}_i, \mathcal{P}_j)$ for all $j \geq i$. Edges between $(\mathcal{P}_h, \mathcal{P}_i)$ for $h < i$ are not required as $\mathcal{P}_h$ has already been reintroduced and solved by this point. As such, loading only the i'th row of Γ in its upper triangle is sufficient.

Fig. 3 provides an example state of the blocked edge-matrix and the contraction of a partition.

[4] This statement is not quite true for vertices in $\mathcal{P}_i$ forming sub-paths within paths. However, for one endpoint of the sub-paths, the path ID and the rank have been computed at this point, and these values are propagated to the rest of the sub-path.

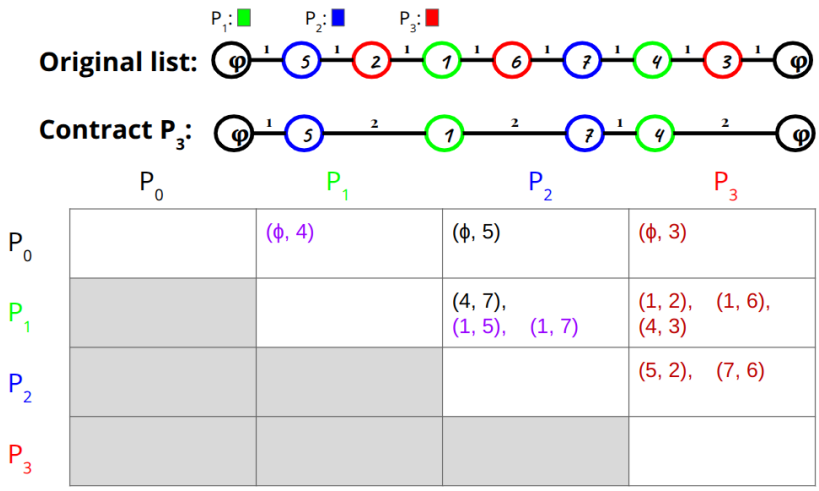

Fig. 3: Upper-triangular edge-matrix for an example discontinuity graph Γ with only one maximal path (list), and a single contraction step. Red entries correspond to edges incident to P_3. These are "merged" when contracting P_3, resulting into the purple entries introduced to Γ.

Collation of the Local Maximal Unitigs After the expansion of contracted Γ, the path ID and the rank of each original edge of Γ have been computed. These pieces of information reside in different cells of the blocked edge-matrix. For an original path $p = (v_0, e_1, v_1, \ldots, v_n, e_{n+1}, v_{n+1})$, e_i's information is in the cell $(\mathfrak{P}(v_{i-1}), \mathfrak{P}(v_i))$ of Γ (or in the transpose cell). The e_i's need to be collated together from the different cells in their proper rank, and their labels then concatenated, to produce the corresponding maximal unitig of p. We perform this with a *MapReduce*-like [10] scheme. For each original edge $e = (_, 1, s)$ with $\texttt{path}(e) = \pi$, $\texttt{rank}(e) = \rho$, and label s, we consider π as its key and (ρ, s) as its value. Edges with the same key are *mapped* to the same bucket, and each bucket is then *reduced* to bring all the edges with the same key in it together in their appropriate rank.

We allocate a list KV of η external-memory buckets for the original edges. For each original edge $e = (_, 1, s)$ in parallel, we map e's path information (π, ρ) and its label s to the bucket $KV_{\xi(\pi)}$, where $\xi : \Sigma^k \to [1, \eta]$ is a uniform hash function. Then for each bucket KV_i in parallel, we reduce it: we sort KV_i by the key (π, ρ), which brings together all the labels with the same π-value in their ρ-order. Concatenating the labels s with the same π-value in this order produces the maximal unitigs of G that span multiple subgraphs.

2.4 Colors Extraction

The colored de Bruijn graph adds an inverted index structure to the graph: each vertex is associated to its *color* and thus maps back to all the input sources in which it is contained. To extract the colors of all the vertices, the scheme used in existing methods [9,15,25] is to collect all the pairs (v, s) such that the vertex (i.e. k-mer) v appears in source s, then to sort these pairs to collate the sources of each vertex. Each k-mer instance from the input constitutes a pair in this approach. At scale, this entails sorting substantial amounts of data, either as a whole [15,25], or in parts [9,1].

In Cuttlefish 3, we introduce a novel method for collecting the unique colors of a graph and associating the vertices to these sets. We avoid collecting the color information for the entire vertex set, and instead propose a scheme to collect the colors for only a *sparse* subset of the vertices, from which the colors of the remaining vertices can be directly inferred based on the contracted form of each subgraph $\mathcal{G}_i$. During the construction and contraction of $\mathcal{G}_i$ (see Sec. 2.2), a subset Υ_i of its vertices are identified as of interest. These are the vertices where the maximal unitig walks encounter shifts in colors [5]: for each subpath p with the same color c in a maximal unitig, only the first vertex v is added to Υ_i. If c can be extracted for v, then the color of the entirety of p is available. However, this forms a causality dilemma—we need to identify the shifts in colors in $\mathcal{G}_i$'s maximal unitigs in order to construct Υ_i, so that $\mathcal{G}_i$'s vertices' colors can be collected.

[5] Including the first vertex in the walk.

To address this, we use the fact that we only need to detect the *shifts* in colors in a maximal unitig to construct Υ_i, and not the colors themselves. For a color $c = \{j_1, \ldots, j_n\}$, we define its *signature* as $h(c) = h''(h'(j_1), \ldots, h'(j_n))$: h' is a hash function for the source-ID j's and h'' is an *online* [6] hash function to combine h''s values.

During the construction of $\mathcal{G}_i$, h'' being online enables us to compute $h(c)$ for each vertex v in $\mathcal{G}_i$, without having its full color c present. During partitioning (Sec. 2.1) we associate to each edge e the source ID j from which it originated. Then while constructing $\mathcal{G}_i$ (Sec. 2.2), for each edge-source pair $(e = \{u, v\}, j)$, the color signatures associated to the vertices u and v are updated online with $h'(j)$. [7]

During the contraction of $\mathcal{G}_i$, as each maximal unitig p is constructed, a walk over p provides the vertices where $h(c)$ shifts. The set of unique colors across the whole graph G is tracked with a concurrent hashtable $\mathcal{C}$, which maps a color signature $h(c)$ to the coordinate (or pointer) of c in the color-output. For a color-shifting vertex v in p, if its $h(c)$ is not found in $\mathcal{C}$, then it is added to Υ_i as a vertex of interest. Otherwise, c's coordinate in the color-output (available from $\mathcal{C}$) is associated to v's position in p.

After the contraction of $\mathcal{G}_i$, all vertices in $\mathcal{G}_i$ that are color-shifting *and* have their colors absent in C are identified and present in Υ_i. Then we scan the edge-source pairs $(e = \{v_0, v_1\}, j)$ of $\mathcal{G}_i$ again, and for each v found to be in Υ_i, we add the key-value pair (v, j) to an external-memory collection. It is then semi-sorted with a *counting sort*-like method to group together pairs with the same keys—the values in a group with the key v constitute v's color c. c is added to the color-output, and the key $h(c)$ is added to $\mathcal{C}$ with c's coordinate in the output as its value. We also associate this color-coordinate back to v's position in its maximal unitig p (these positions are tracked separately).

Finally, when the locally maximal unitigs are collated (Sec. 2.3), their colors are also gathered and collapsed if required—consecutive unitigs can continue sub-paths with the same color.

Fig. 4 illustrates an example of the color signatures and how these are computed online.

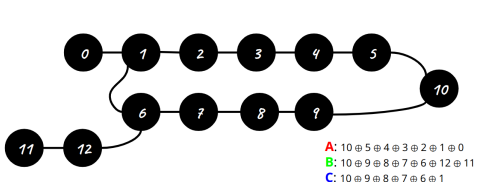

(a) The subgraph with no color-information added to it yet.

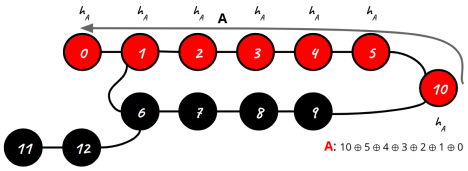

(b) Sequence A's vertices added and their color signatures updated with A's hash, h_A.

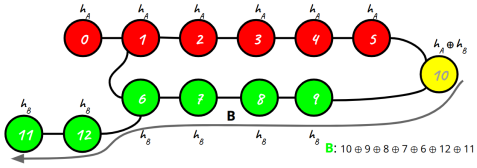

(c) Sequence B's vertices added / updated and their color signatures updated with B's hash, h_B.

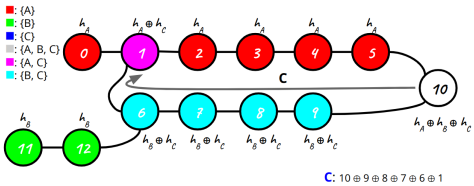

(d) Sequence C's vertices updated with C's hash, h_C.

Fig. 4: A subgraph constructed from three sequences A (red), B (green), and C (blue). The sequences are denoted as concatenations of vertices (k-mers). The figures show how, during the construction of the subgraph, its vertices' color signatures (color-coded visually) get updated. The vertices have no color-information at the beginning, color-coded as black. Then the sequences A, B, and C are traversed in order. With each vertex seen during the walks of the sequences, its color signature is updated online. Finally, the complete color signature is available for each vertex.

[6] The entire set of $h'(j)$'s is not required to be available simultaneously to compute h''.

[7] A vertex being present in the same source s_j multiple times presents a fundamental barrier to the online nature of h'' and, as a result, to the uniqueness of $h(c)$ from different multiset variants of c—see Sec. 3.3.

Asymptotics We briefly discuss the running times of the different phases of the algorithm. For an input set $\mathcal{S}$, let its total size be $\ell = \sum_{s \in \mathcal{S}} |s|$, the number of vertices (unique k-mers) and edges (unique $(k+1)$-mers) in the de Bruijn graph G be n and m respectively, and the number of vertices in the discontinuity graph Γ be γ. The partitioning step makes one pass over each $s \in \mathcal{S}$, touching each k-mer instance once, requiring $\mathcal{O}(\ell)$ work. Next, constructing a subgraph $\mathcal{G}_i$ requires scanning over $\mathcal{G}_i$'s edges (or groups of edges through super k-mers), as many times as they are present in the input—in total amounting to another scan over the input, $\mathcal{O}(\ell)$. Then the contraction of $\mathcal{G}_i$ traverses it once, requiring $\mathcal{O}(n+m)$ work in total. Then we process (contract and then expand) Γ, where each vertex and its incident edges are processed twice—once during contraction and once during expansion. Also, each maximal path p in Γ produces $(|p|-1)$ new edges during contraction, summing to $\mathcal{O}(\gamma)$ new edges. In total, these steps require work $\mathcal{O}(\gamma)$. Collation of the locally maximal unitigs involve moving them to appropriate buckets and to semi-sort them. Since they sum to $(n+\gamma)$ in size, this step requires $\mathcal{O}(n)$ work.

3 Algorithm Optimization

We discuss some of the salient optimizations and implementation details that have been critical to optimize Cuttlefish 3's performance in this section.

3.1 Branch-Free Minimizer Computation

Instead of distributing the edges to subgraphs piecewise, we group together consecutive edges in the input as maximal super k-mers [21], similar to [9,7]. Given a string s, splitting it into maximal super k-mers requires computing the minimizer of each constituent k-mer. Computing the ℓ-minimizer of a k-mer takes time $\mathcal{O}(k-\ell)$. Naively computing all minimizers in s takes time $\mathcal{O}\big(|s|(k-\ell)\big)$. This is typically improved to amortized time $\mathcal{O}(|s|)$ as following. The k-mers of s are scanned, while a deque q of ℓ-mers is maintained. q stores a subset of the ℓ-mers of the current k-mer, that are *candidate* minimizers for k-mers yet to be scanned. Each subsequent k-mer v introduces a new ℓ-mer x to q, while the oldest ℓ-mer z in q, if out of range of x, is removed from q. q is maintained sorted—all ℓ-mers $y > x$ in q are popped off as they cannot be the minimizer of v or any next k-mer. The front of q thus contains the minimizer of v. Since each new ℓ-mer x is compared with a variable number of $y \in q$ and the resulting minimizer is available only after such comparisons, this method can induce many *branches* in the generated processor instructions.

Instead, we simply maintain an ordered list M of all the ℓ-mers of the current k-mer, and compute the minimum of M for each k-mer. Computing the minimum of M from scratch takes time $\mathcal{O}(k-l)$, but we reuse the computations for subsequent k-mers. A k-mer has $(k-\ell+1)$ ℓ-mers, and two consecutive k-mers u and v share $(k-\ell)$ ℓ-mers. Say the list of the last $(k-\ell)$ ℓ-mers of u is M_u. v has just one new ℓ-mer y apart from M_u. If we know $x = \min(M_u)$, then v's minimizer computation is just $\min(x, y)$—a single computation doable without branches.

We partition M into two windows: L and R. L is at the front of M while R is at the back. Initially, $L = M$ and R is empty. So $\min(M) = \min(L)$. For each new k-mer v, an ℓ-mer y is appended to R, while one ℓ-mer falls out of L's prefix. So a suffix L_{suf} of the initial L and the entire current R belong to v. We construct a suffix-min table for the initial L, computed at the beginning, from which $\min(L_{suf})$ is available. We also maintain the running $\min(R)$, updated with every new addition to it. Thus the minimizer of v is $\min\big(\min(L_{suf}), \min(R)\big)$. This computation is branch-free.

When L becomes empty, we reset the data structures: L and R are swapped [8], and we recompute the suffix-min table of L. This computation has one linear scan computing a running minimum, which introduces some conditional dependence among instructions. This can be minimized with vectorization.

The suffix-min table computation takes time $\mathcal{O}(k-l+1)$, happening at every $(k-l+1)$'th k-mer. Thus the total time to compute all the minimizers is $\mathcal{O}(|s|)$, and each takes amortized constant time.

[8] L and R are conceptual—all computations are directly over M.

3.2 Cache-friendly Subgraph Atlases / B-tree

With a separate subgraph for each ℓ-minimizer, we have to maintain 4^ℓ subgraphs. With practical values of ℓ, handling many external-memory buckets posees bottlenecks with the filesystem. So we group together minimizers into a smaller number of subgraphs through uniform hashing.

It is also preferable to have a large enough number g of subgraphs such that the subgraph sizes are small enough to avoid large in-memory representations. In a parallel implementation with w workers, each subgraph bucket should have w worker-local buffers of super k-mers so as to minimize lock-contention for the subgraph. This results in $g \times w$ buffers in-memory, and the end of each are contending for space in cache. To improve caching behavior, we group together subgraphs into atlases (similar to texture-atlases [27]). We keep $\sqrt{g}$ atlases. Super k-mers are added to the atlases, instead of directly to the subgraphs, so that we maintain only $\sqrt{g} \times w$ buffers in memory. Only when a buffer fills up are its super k-mers distributed to the $\sqrt{g}$ subgraphs in the atlas [9]. In that case, an additional $\sqrt{g}$ buffers' ends come into the cache. Note that this scheme is similar to having a *B-tree* of the subgraphs.

3.3 Color-signatures for Multisets

Defined in Section 2.4, the signature of a color c is $h(c) = h''\big(h'(j_1), \ldots, h'(j_n)\big)$—it is a hash-combination of the hash values of $j \in c$. A vertex v can belong to the same source s_j multiple times, and as such, its color c will be observed in a multiset variant in this case. Thus $h'(j)$ will be combined to $h(c)$ multiple times. h'' being online and memoryless, the color c can have different signatures for the different variants of c. This makes it impossible to correctly identify the color-shifts.

To tackle this, we process the input sources in a consistent order, so that the subgraph buckets contain their super k-mers in that order. As a result, any multiset variant of c is always observed in sorted order. Each vertex v in $\mathcal{G}_i$ keeps track of the last source ID j added to its $h(c)$, and if j is added again to it, we simply skip it. This ensures that all multiset variants of c produce the same $h(c)$.

3.4 Color Encoding

Even when deduplicated into *color-equivalence classes* [3], the collection of distinct colors can be very large, requiring a substantial amount of on-disk space. In fact, efficient representations of related colors has received considerable attention [22,26,12,2,18]—yet most of that work focuses on the indexing problem, where all of the potential colors are known ahead of time, and can be arbitrarily arranged and inspected during compression. To reduce the size of the the stored colors, Cuttlefish 3 adopts the encoding scheme introduced in Fulgor [13]. Specifically, this *hybrid* encoding first determines the density of the color (the ratio of sources present in the set to the total number of input sources). We then choose one of three different representations based on this density for each unique color. For colors considered sparse (density < 0.25), we δ-encode the list and then use Elias' universal δ-code [11] to represent the first source ID and the subsequent gaps between the IDs in the list. For colors considered dense (density > 0.75), we first *complement* the list, i.e. record instead the set of colors *not* present in the color, and encode the complement list using the aforementioned strategy. Finally, for colors with intermediate density (i.e. ≥ 0.25 and ≤ 0.75), we encode the color as a dense bit-vector. For all the encodings, the first element of the encoding is an Elias δ-encoded integer recording the number of colors in the *original* color.

4 Results

We evaluate the performance characteristics of Cuttlefish 3 and how it compares to the state-of-the-art solution GGCAT [9] in constructing (colored) compacted de Bruijn graphs in this section.

Experiments were performed on a single machine with four Intel(R) Xeon(R) Platinum 8160 2.10GHz CPUs having 96 cores in total, 1.5 TBs of 2.66 GHz DDR4 RAM, and two 3.5 TBs Toshiba PX05SRB384Y ATA SSDs. The running times and the maximum memory usages were measured with the GNU `time` command.

[9] Through an atlas-central buffer instead of direct addition, to further reduce this occurrence.

The evaluated tools were restricted to CPU-usages concording to the number of threads with the `cpulimit` tool[10].

4.1 Datasets

The experiments are performed on the following datasets: (1) Human gut [14]: 30,691 representative sequences from prevalent human gut prokaryotic genomes (≈ 61B bp, 18 GB gzipped FASTA); (2) Iowa corn [16]: a soil metagenome read set from 100-years-cultivated Iowa agricultural corn soil (≈ 208B bp, SRX100357 and SRX099904–06, 152 GB gzipped FASTQ); (3) Salmonella (309K): 309,123 *Salmonella* genome sequences used in [9], downloaded from the *EnteroBase* database (≈ 1.5T bp, 1.36 TB FASTA); and (4) Bacterial archive [5]: 661,405 bacterial genomes (≈ 2.58T bp 757 GB gzipped FASTA).

4.2 Compacted de Bruijn Graph Construction

We evaluate Cuttlefish 3 against GGCAT for two realistic values of k used with de Bruijn graphs in practice: 31 and 63, and skip impractical larger values. [9] demonstrates that GGCAT outperforms Cuttlefish 2 in this use-case, which in turn outperforms other leading methods, Bifrost, and BCALM 2, demonstrated in [19]. Hence we do not compare against Cuttlefish 2, Bifrost, and BCALM 2. The results are available in Table 1. We validated the constructed maximal unitigs from various subsets of the bacterial archive to the ones produced from Cuttlefish 2 [19] for correctness.

Table 1: Time (in wall clock) and memory (in GB, in parentheses) performance results for constructing compacted de Bruijn graphs. The best performance-metrics in each row are highlighted.

k	Dataset	Threads	GGCAT	Cuttlefish 3
31	Human gut	16	17 m (**5.4**)	**13 m** (8.2)
		32	10 m (**9.5**)	**08 m** (13.5)
	Iowa corn	16	49 m (**14.5**)	**41 m** (15.6)
		32	30 m (26.0)	**26 m** (**24.0**)
	Salmonella (309K)	16	01 h 52 m (8.4)	**01 h 21 m** (**4.2**)
		32	01 h 02 m (10.8)	**43 m** (**6.1**)
	Bacterial archive (661K)	16	04 h 43 m (**9.4**)	**03 h 05 m** (11.5)
		32	02 h 32 m (**14.6**)	**01 h 44 m** (18.7)
63	Human gut	16	16 m (7.3)	**14 m** (**8.2**)
		32	**10 m** (12.0)	**08 m** (**13.6**)
	Iowa corn	16	**23 m** (**6.9**)	**23 m** (11.0)
		32	15 m (**12.1**)	**14 m** (16.0)
	Salmonella (309K)	16	01 h 45 m (8.4)	**01 h 14 m** (**4.1**)
		32	59 m (10.7)	**39 m** (**5.9**)
	Bacterial archive (661K)	16	04 h 08 m (**9.6**)	**02 h 50 m** (11.9)
		32	02 h 13 m (**14.0**)	**01 h 43 m** (19.6)

From Table 1, we observe that for each dataset, Cuttlefish 3 is faster than GGCAT. For the relatively smaller datasets of human gut genomes and Iowa corn reads, Cuttlefish 3 performs similar to GGCAT. On the larger datasets however, Cuttlefish 3 is achieves significant speedup over GGCAT. On the tested configurations, it is 1.38–1.51× faster on the Salmonella dataset. On the bacterial archive, it is 1.29–1.53× faster. In all the cases, Cuttlefish 3 has a memory-profile similar to that GGCAT.

4.3 Colored Compacted de Bruijn Graph Construction

We evaluate Cuttlefish 3 compared to GGCAT with $k = 31$ to construct the colored de Bruijn graph on the genome sequence datasets. [9] demonstrates that GGCAT is more efficient than Bifrost for this use-case and as such we do not compare against it. Table 2 contains the benchmark results.

[10] We adopt `cpulimit` as we noticed that GGCAT, during extended executions, uses up to 175% of the thread resources requested by the user.

Table 2: Time (in wall clock) and memory (in GB, in parentheses) performance results for constructing colored compacted de Bruijn graphs. The best performance-metrics in each row are highlighted.

k	Dataset	Threads	GGCAT	Cuttlefish 3
31	Human gut	16	25 m (**15.1**)	**19 m** (19.1)
		32	17 m (**19.0**)	**11 m** (25.2)
	Salmonella (150K)	16	02h 07 m (7.9)	**01 h 19 m** (**7.4**)
		32	01 h 08 m (**10.3**)	**42 m** (**10.3**)
	Salmonella (309K)	16	04 h 51 m (11.7)	**02 h 53 m** (**10.8**)
		32	02 h 34 m (**14.2**)	**01 h 32 m** (15.9)
	Bacterial archive (661K)	16	09 h 59 m(29.0)	**06 h 02 m** (**28.4**)
		32	05 h 10 m (36.1)	**03 h 18 m** (**33.7**)
63	Human gut	16	22 m (16)	**18 m** (**14.2**)
		32	15 m (20.7)	**11 m** (20.4)
	Salmonella (150K)	16	02h 01 m (8.1)	**01 h 14 m** (**7.7**)
		32	01 h 05 m (**10.4**)	**39 m** (11)
	Salmonella (309K)	16	04 h 33 m (12.25)	**02 h 47 m** (**11.3**)
		32	02 h 21 m (**14.6**)	**01 h 30 m** (17.5)
	Bacterial archive (661K)	16	08 h 41 m (30.6)	**05 h 40 m** (**28.5**)
		32	04 h 30 m (**38.7**)	**03 h 15 m** (41.3)

From Table 2, we note that Cuttlefish 3 is significantly faster than GGCAT for all the datasets. For $k = 31$, on 150K Salmonella genomes, Cuttlefish 3 is ≈1.61× faster than GGCAT. For 309K Salmonella, Cuttlefish 3 is ≈1.68× faster. On the bacterial archive (661K), it is 1.57–1.65× faster than GGCAT. The relative performance differences are quite similar at $k = 63$ and he memory usages are comparable across the test configurations.

4.4 Parallel Scaling

We assess the parallel scaling speedup of Cuttlefish 3 across a varying number of processor-threads in this experiment. We use a subset of 10,000 bacteria from the bacterial archive dataset for this. We set $k = 31$, and executed Cuttlefish 3 in both uncolored and colored mode, with thread-counts ranging in 1–32. Figure 5 demonstrates the running times. We also include in this figure an estimated loose lower bound on the minimal time achievable for construction on this dataset at different thread counts. This estimate is obtained by simply measuring the time required to (in parallel) decompress the input files twice, but without performing any parsing. It seems reasonable that any approach—including those using the partition-contract-join paradigm—will have to scan the data at least two times, motivating our proxy measurement for a loose lower bound.

4.5 Sparsification for Color Extraction

In the colored compacted graph construction experiments, we measured the effectiveness of our sparcification strategy (outlined in Section 2.4). Our strategy not only reduces the number of vertices for which the full color needs to be extracted but also exploits the fact that many color-shifting vertices will have identical colors. If a color corresponding to the signature (i.e. hash) of a color-shifting vertex has already been computed and inserted into the color-table, then it is unnecessary to assemble that color again. Table 3 provides some statistics on the degree of sparsification, and thus reduction in overall work, that our strategy enables. We observe that the number of color shifting vertices is usually a small fraction of the total number of vertices (i.e.the graph size). More importantly, even for the vast majority of color shifting vertices, at the time we encounter them, we have already computed the color corresponding to their signature. Thus, across the three datasests in Table 3, we need to compute the colors for only between $0.83\% - 3.78\%$ of the total vertices in the graph.

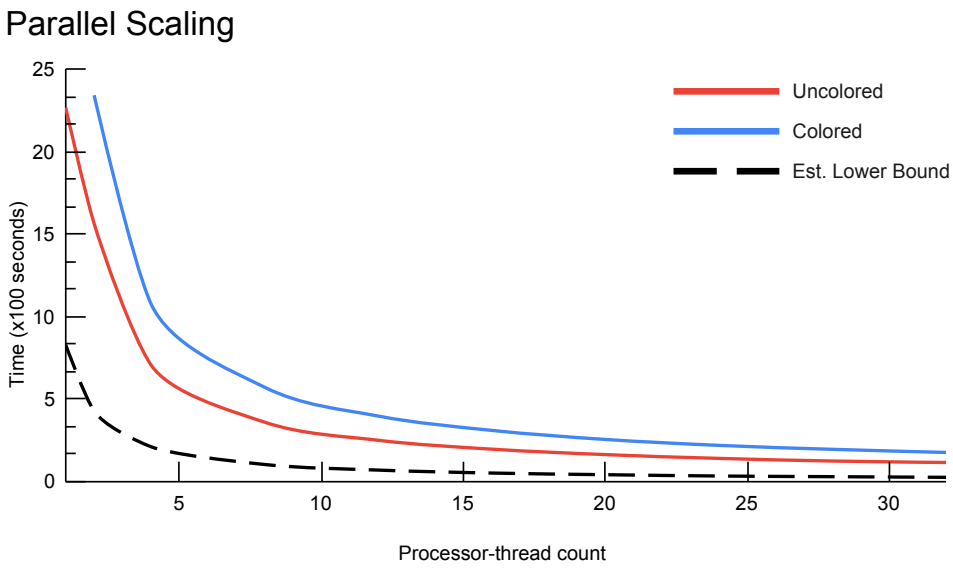

Fig. 5: Time incurred by Cuttlefish 3 across varying processor-thread counts for 10K bacteria.

Table 3: Graph and color related statistics for the datasets for which we construct the ccdBG.

Dataset	Graph-size ($\times 10^9$)	Color-shifting vertex ($\times 10^9$)	Vertices w/ new color-signature ($\times 10^9$)	Percent-age	Pairs sorted ($\times 10^9$)	Colors ($\times 10^6$)
Human gut (31K)	15.33	1.95	0.232	1.51	10.05	227.8
Salmonella (150K)	0.54	0.08	0.019	3.63	478.0	19.3
Salmonella (309K)	0.72	0.109	0.027	3.78	1109.3	27.2
Bacteria (661K)	48.78	5.71	0.404	0.83	1459.8	389.1

5 Conclusion

We have introduced Cuttlefish 3, a fast, parallel, and low-memory algorithm, and its prototype implementation to construct (colored) compacted de Bruijn graphs. It is highly scalable across a cvariety of large-scale genomic datasets. We observed that Cuttlefish 3 constructed the colored compacted graph for massive datasets up-to 1.68× faster than the current state-of-the-art method, GGCAT, with the same memory profile. Cuttlefish 3 reduces Cuttlefish 2's computational requirements substantially by adopting the partition-contract-join paradigm initally introduced by BCALM 2. Moreover, it introduces several novel ideas to this paradigm. Cuttlefish 3 generalizes the vertex-modeling schemes of Cuttlefish 1 and 2 to associate neighborhood states to vertices in subgraphs, which significantly reduces the amount of work to traverse the subgraphs. It makes use of a novel algorithm to stitch together the local solutions from the subgraphs. For colored graphs, it introduces a novel multi-pass scheme to vastly sparsify the set of vertices only for which colors need to actually be track and constructed, which is sufficient for the entire compacted graph. For example, we found that while tracking the colors for only 0.83% of the unique k-mers of the 661K bacterial archive [5], Cuttlefish 3is able to construct the correct colors for all of the vertices.

In addition to the algorithmic improvements, several facets in the implementation of Cuttlefish 3 turned out to provide particularly useful insights. Fast parsing [29] of massive amounts of (compressed) sequences is crucial when dealing with terabytes of data. When partitioning the input sequences to a number of subgraph

buckets, these buckets can grow very large and surpass the input sizes, and as such (de)compressing the buckets on-the-fly is important [9]. For in-memory representation of the subgraphs, more cache-friendly data structures have the potential to yield non-trivial performance improvements. Additionally, disk speeds have substantial impact on this I/O heavy paradigm, since disks are frequently used to batch-in and -out partitions of various data structures throughout. We suspect that fast disks, that admit parallel access, will become increasingly important to enable high-performance bioinformatics applications in the future. Finally, while further improvements, of both an engineering and algorithmic nature are certainly possible, and we are continuing to explore these, we have reason to believe that current best-in-class approaches for (colored) compacted de Bruijn graphconstruction are not far from a reasonable, approximate, practical lower bound on construction time.

Availability. Cuttlefish 3 is implemented in `C++17` and is available at `https://github.com/COMBINE-lab/cuttlefish/tree/cuttlefish3` under the BSD 3-clause license.

Funding. This research has been supported with funding from the US NIH (R01 HG009937), the US NSF (CCF-1750472, CNS-1763680, and SaTC-2,317,194), and the Chan Zuckerberg Initiative DAF (grants 252586 and 2024342821).

Conflict of Interest. RP is a co-founder of Ocean Genomics, inc. The other authors declare that they have no competing interests.

References

1. Fatemeh Almodaresi, Jamshed Khan, Sergey Madaminov, Michael Ferdman, Rob Johnson, Prashant Pandey, and Rob Patro. An incrementally updatable and scalable system for large-scale sequence search using the Bentley–Saxe transformation. *Bioinformatics*, 2022.
2. Fatemeh Almodaresi, Prashant Pandey, Michael Ferdman, Rob Johnson, and Rob Patro. An Efficient, Scalable, and Exact Representation of High-Dimensional Color Information Enabled Using de Bruijn Graph Search. *Journal of Computational Biology*, 2020.
3. Fatemeh Almodaresi, Prashant Pandey, and Rob Patro. Rainbowfish: A Succinct Colored de Bruijn Graph Representation. 2017.
4. Richard J. Anderson and Gary L. Miller. A simple randomized parallel algorithm for list-ranking. *Information Processing Letters*, 1990.
5. Grace A. Blackwell, Martin Hunt, Kerri M. Malone, Leandro Lima, Gal Horesh, Blaise T. F. Alako, Nicholas R. Thomson, and Zamin Iqbal. Exploring bacterial diversity via a curated and searchable snapshot of archived DNA sequences. *PLOS Biology*, 2021.
6. Rayan Chikhi, Antoine Limasset, Shaun Jackman, Jared T. Simpson, and Paul Medvedev. On the representation of de bruijn graphs. In *Research in Computational Molecular Biology*, 2014.
7. Rayan Chikhi, Antoine Limasset, and Paul Medvedev. Compacting de Bruijn graphs from sequencing data quickly and in low memory. *Bioinformatics*, 2016.
8. Rayan Chikhi and Guillaume Rizk. Space-efficient and exact de bruijn graph representation based on a bloom filter. *Algorithms for Molecular Biology*, 2013.
9. Andrea Cracco and Alexandru I Tomescu. Extremely fast construction and querying of compacted and colored de bruijn graphs with GGCAT. *Genome Res.*, 2023.
10. Jeffrey Dean and Sanjay Ghemawat. MapReduce: Simplified data processing on large clusters. In *OSDI*, 2004.
11. Peter Elias. Efficient Storage and Retrieval by Content and Address of Static Files. *Journal of the ACM*, 1974.
12. Jason Fan, Jamshed Khan, Noor Pratap Singh, Giulio Ermanno Pibiri, and Rob Patro. Fulgor: a fast and compact k-mer index for large-scale matching and color queries. *Algorithms for Molecular Biology*, 2024.
13. Jason Fan, Jamshed Khan, Noor Pratap Singh, Giulio Ermanno Pibiri, and Rob Patro. Fulgor: a fast and compact k-mer index for large-scale matching and color queries. *Algorithms for Molecular Biology*, 2024.
14. Pranvera Hiseni, Knut Rudi, Robert C. Wilson, Finn Terje Hegge, and Lars Snipen. HumGut: a comprehensive human gut prokaryotic genomes collection filtered by metagenome data. *Microbiome*, 2021.
15. Guillaume Holley and Páll Melsted. Bifrost: highly parallel construction and indexing of colored and compacted de Bruijn graphs. *Genome Biology*, 2020.

16. Adina Chuang Howe, Janet K. Jansson, Stephanie A. Malfatti, Susannah G. Tringe, James M. Tiedje, and C. Titus Brown. Tackling soil diversity with the assembly of large, complex metagenomes. *Proceedings of the National Academy of Sciences*, 2014.
17. Shaun D Jackman, Benjamin P Vandervalk, Hamid Mohamadi, Justin Chu, Sarah Yeo, S Austin Hammond, Golnaz Jahesh, Hamza Khan, Lauren Coombe, Rene L Warren, and Inanc Birol. ABySS 2.0: resource-efficient assembly of large genomes using a Bloom filter. *Genome Res.*, 2017.
18. Mikhail Karasikov, Harun Mustafa, Amir Joudaki, Sara Javadzadeh-no, Gunnar Rätsch, and André Kahles. Sparse Binary Relation Representations for Genome Graph Annotation. *Journal of Computational Biology*, 2020.
19. Jamshed Khan, Marek Kokot, Sebastian Deorowicz, and Rob Patro. Scalable, ultra-fast, and low-memory construction of compacted de bruijn graphs with Cuttlefish 2. *Genome Biology*, 2022.
20. Jamshed Khan and Rob Patro. Cuttlefish: fast, parallel and low-memory compaction of de Bruijn graphs from large-scale genome collections. *Bioinformatics*, 2021.
21. Yang Li, Pegah Kamousi, Fangqiu Han, Shengqi Yang, Xifeng Yan, and Subhash Suri. Memory efficient minimum substring partitioning. *Proc. VLDB Endow.*, 2013.
22. Camille Marchet, Christina Boucher, Simon J Puglisi, Paul Medvedev, Mikaël Salson, and Rayan Chikhi. Data structures based on k-mers for querying large collections of sequencing data sets. *Genome Res.*, 2021.
23. Gary L. Miller and John H. Reif. Parallel tree contraction part 1: Fundamentals. In *Randomness and Computation*, pages 47–72. 1989. Vol. 5.
24. Ilia Minkin, Son Pham, and Paul Medvedev. TwoPaCo: an efficient algorithm to build the compacted de Bruijn graph from many complete genomes. *Bioinformatics*, 2016.
25. Prashant Pandey, Fatemeh Almodaresi, Michael A. Bender, Michael Ferdman, Rob Johnson, and Rob Patro. Mantis: A fast, small, and exact large-scale sequence-search index. *Cell Systems*, 2018.
26. Giulio Ermanno Pibiri, Jason Fan, and Rob Patro. *Meta-colored Compacted de Bruijn Graphs.* 2024.
27. Budirijanto Purnomo, Jonathan D. Cohen, and Subodh Kumar. Seamless texture atlases. In *SIGGRAPH*, 2004.
28. Jim Wyllie. The complexity of parallel computations. 1979.
29. Hao Zhang, Honglei Song, Xiaoming Xu, Qixin Chang, Mingkai Wang, Yanjie Wei, Zekun Yin, Bertil Schmidt, and Weiguo Liu. RabbitFX: Efficient Framework for FASTA/Q File Parsing on Modern Multi-Core Platforms. *IEEE/ACM Transactions on Computational Biology and Bioinformatics*, 2023.
30. Hongyu Zheng, Guillaume Marçais, and Carl Kingsford. Creating and using minimizer sketches in computational genomics. *Journal of Computational Biology*, 2023.